

Fluid particle dynamics simulation of charged colloidal suspensions

This article has been downloaded from IOPscience. Please scroll down to see the full text article.

2004 J. Phys.: Condens. Matter 16 L115

(<http://iopscience.iop.org/0953-8984/16/10/L01>)

View [the table of contents for this issue](#), or go to the [journal homepage](#) for more

Download details:

IP Address: 129.252.86.83

The article was downloaded on 27/05/2010 at 12:48

Please note that [terms and conditions apply](#).

LETTER TO THE EDITOR

Fluid particle dynamics simulation of charged colloidal suspensions

Hiroya Kodama¹, Kimiya Takeshita¹, Takeaki Araki² and Hajime Tanaka²

¹ Mitsubishi Chemical Group Science and Technology Research Centre Incorporated, Yokohama 227-8502, Japan

² Institute of Industrial Science, University of Tokyo, Meguro-ku, Tokyo 153-8505, Japan

E-mail: kodama@rc.m-kagaku.co.jp and tanaka@iis.u-tokyo.ac.jp

Received 13 February 2004

Published 27 February 2004

Online at stacks.iop.org/JPhysCM/16/L115 (DOI: 10.1088/0953-8984/16/10/L01)

Abstract

A new method of simulation of the dynamics of charged colloidal suspensions is formulated that is based on the fluid particle dynamics method (Tanaka and Araki 2000 *Phys. Rev. Lett.* **85** 1338) so as to incorporate the electrohydrodynamic interactions properly. The fluid particle approximation allows us to treat dynamic coupling among motions of the three relevant elements of charged colloidal suspensions, i.e., colloidal particles, ion clouds, and liquid, in a physically natural manner. The validity of our method is demonstrated for a problem of the electrophoretic deposition of charged colloids. Our simulation results clearly indicate that the electro-osmotic flow causes 'effective' long-range attractions between charged particles of the same sign, as previously suggested by experiments and theories.

Liquid suspensions containing colloids are of fundamental importance in soft matter physics, surface chemistry, biology, and industry [1–3]. In colloidal suspensions, charges play key roles in stabilizing the dispersions and also in electrically manipulating suspended particles. It is also widely known that they affect various kinetic phenomena of colloidal suspensions, such as sedimentation, rheology, and electrophoresis. When one tries to study the dynamics of charged colloidal suspensions either theoretically or numerically, the most difficult problem arises from the complex dynamic coupling among motions of the three key elements; that is, colloidal particles, ions, and liquid molecules. These elements are strongly interacting with each other via both electrostatic and hydrodynamic interactions. Since these static and dynamic interactions are both of long-range nature, we must inevitably deal with a very complex dynamic many-body problem. Because of these difficulties, there have so far been neither theoretical nor numerical studies that take into account the full static and dynamic coupling among the motions of these three key elements of colloidal suspensions, despite the scientific

and industrial importance. In most previous methods, the motion of one of these elements has to be dropped somehow, as will be briefly reviewed below.

Molecular dynamics (MD) simulation is a straightforward method for incorporating hydrodynamic and electrostatic interactions by explicitly solving for the motions of colloids, ions, and liquid molecules. In principle, thus, MD simulation can be a quite powerful means for studying the dynamic behaviour of charged colloidal suspensions, in particular, the short-time behaviour and the local charge ordering. In reality, however, it is too costly for dealing with the hydrodynamic motion of liquid molecules and the resulting motion of colloids and ions. Thus, liquid molecules have so far been neglected. To improve this situation, Tanaka and Grosberg [4] conducted a new type of MD simulation to estimate the electrophoretic mobility of a single charged particle. In this work, the hydrodynamic effect of liquid molecules is incorporated by explicitly dealing with many neutral particles along with ions. Although this is an important step toward the inclusion of full hydrodynamic effects, MD simulation is obviously not suitable for dealing with many colloidal particle systems because of the large time separation between the motion of colloidal particles and that of ions and liquid and the resulting enormous computational cost. Thus, the number of colloidal particles and the timescale have to be limited. It should be noted that hydrodynamic interactions between particles play crucial roles in the large-spatial-scale and long-timescale phenomena. Coarse graining of the problem is, thus, essential.

Eliminating the degrees of freedom of ions and/or liquid molecules is a possible way to improve the efficiency of simulation. Hydrodynamic interactions between colloidal particles were incorporated by Stokesian dynamics [5, 6], which calculates the mobility matrix for particle motion. Application of this method to charged colloidal problems can be carried out, while keeping a sufficient numerical efficiency, by approximating electrostatic interactions by an effective interparticle potential such as the Yukawa potential [7]. Although this can be a quite efficient method, obviously the possible change in the spatial ion distribution cannot be investigated by this method.

There are also efforts to incorporate many-particle features in an approximate manner. For example, properties dependent upon particle concentration were discussed by considering a single particle fixed in a cell with adequate boundary conditions and varying the cell size such that the particle/cell volume ratio is equal to the particle volume fraction. Ohshima derived a theoretical expression for electrophoretic mobility of colloidal particles in concentrated suspensions using the cell model [8]; for a system where a single particle is fixed at the centre of a spherical cell, the fluid velocity under an electric field was solved for. Horbach and Frenkel [9] applied the lattice Boltzmann method (LBM) to a system of charged colloids suspended in an electrolyte solution and estimated the effective sedimentation velocity by solving for the gravity-induced flow of an electrolyte solution about a charged particle fixed in a cubic cell with a periodic boundary condition. Although these methods can pick up some important features of colloidal suspensions with a finite particle concentration, the relative motion of the particles and the effects of the resulting hydrodynamic flow are completely neglected.

In all these examples, hydrodynamic interactions between particles are the most serious obstacle due to the dynamic and long-range nature. They induce strong nonlocal couplings among all the relevant degrees of freedom of charged colloidal suspensions. To get rid of the difficulty associated with many-body hydrodynamic interactions among solid particles, a new simulation method (the fluid particle dynamics (FPD) method) was recently proposed for charge-free colloidal suspensions by Tanaka and Araki [10]. Here liquid molecules are treated as a continuum fluid. A key feature of this method is regarding a solid colloidal particle as an undeformable fluid one of high viscosity. It is assumed that viscosity changes smoothly

across the interface between the inner and the outer regions of each particle. Thus, we can get rid of the solid–fluid boundary condition, which is the origin of all the difficulties. This smooth interface approximation allows us to treat the whole colloidal system as a continuous liquid with inhomogeneity of the viscosity, which exactly reflects the spatial distribution of colloidal particles. Because of this feature of the FPD method, all types of hydrodynamic motion of particles are naturally reproduced so as to minimize the viscous dissipation³. In the fluid particle approximation, the spatial distribution of the surface charges of colloidal particles can also be expressed as a continuous field variable⁴. Thus, the FPD method can naturally be extended to incorporate electrohydrodynamic equations. In this letter, we present a novel method of simulation of the dynamics of charged colloidal suspensions based on the FPD method; this method can deal with the full static and dynamic coupling among colloidal particles, ion clouds, and liquid. The continuity of the variables throughout the whole system makes the simulation quite efficient. The validity of our method will be demonstrated for a problem of electrophoretic deposition of charged colloids.

In the following, we explain our new simulation method. The variables relevant for physically describing the dynamics of charged colloidal suspensions are the colloidal particle position $\{\vec{r}_i\}$, the ion distribution $\{C_\alpha\}$, and the fluid velocity field \vec{v} . The indices i and α stand for individual particle and ion type, respectively. We also denote the electrostatic potential as Ψ . In the fluid particle approximation, we regard the solid particles as fluid ones. We express fluid particle i using a function $\phi_i(\vec{r})$ as $\phi_i(\vec{r}) = [\tanh\{(a - |\vec{r} - \vec{r}_i|)/\xi\} + 1]/2$, where a is the radius of the particle and ξ is the interfacial width. For the distribution of the particles given by $\{\vec{r}_i\}$, the viscosity field can be expressed as $\eta(\vec{r}) = \eta_s + \sum_i (\eta_c - \eta_s)\phi_i(\vec{r})$, where η_s is the viscosity of the fluid surrounding particles and η_c is the viscosity inside the particle. Then the time evolution of \vec{v} is described by the Navier–Stokes equation,

$$\rho \frac{D\vec{v}}{Dt} = \vec{F} - \vec{\nabla} p + \vec{\nabla} \cdot \eta\{\vec{\nabla}\vec{v} + (\vec{\nabla}\vec{v})^T\} + \vec{\zeta}, \quad (1)$$

where $\frac{D}{Dt} = \frac{\partial}{\partial t} + \vec{v} \cdot \vec{\nabla}$, ρ is the density, and $\vec{\zeta}$ is the thermal force noise. In the above, we assume that the density of colloidal particles is the same as that of a liquid so that ρ is a constant. Pressure p is determined such that it satisfies the incompressibility condition $\vec{\nabla} \cdot \vec{v} = 0$. In the FPD method, the force $\vec{F}_i^{(0)}$ acting on particle i is transformed into the continuous force field $\vec{F}(\vec{r}) = \vec{F}_i^{(0)}\phi_i(\vec{r})/\int d\vec{r}\phi_i(\vec{r})$, which should be included in \vec{F} in equation (1). The time evolution of the position of particle i , \vec{r}_i , is described by the average fluid velocity inside the particle, $\langle \vec{v} \rangle_{\vec{r}_i} = \int d\vec{r} \vec{v}\phi_i/\int d\vec{r}\phi_i$, as

$$\frac{d\vec{r}_i}{dt} = \langle \vec{v} \rangle_{\vec{r}_i}. \quad (2)$$

This is the framework of the original FPD model. It should be noted that the fluid particle approximation becomes exact in the limit of $\eta_c/\eta_s \rightarrow \infty$ and $\xi/a \rightarrow 0$.

Now we introduce charges into the above model. Let us assume that the valence of ions of type α with the concentration C_α is given by Z_α . We define the charge density localized in the surface region of particle i having the total charge Q_i as $\rho_i(\vec{r}) = Q_i\varphi_i(\vec{r})/\int d\vec{r}\varphi_i(\vec{r})$, where $\varphi_i = \cosh^{-4}\{(a - |\vec{r} - \vec{r}_i|)/\xi\}$ is a function having a value only in the interfacial region of particle i . The total charge density is then expressed as

$$\rho_e = \sum_i \rho_i + \sum_\alpha eZ_\alpha C_\alpha, \quad (3)$$

³ For example, FPD method can describe both translational and rotational hydrodynamic motion of particles properly.

⁴ Since we use the continuous field for the surface charge of a colloidal particle and the ion clouds, our model cannot deal with problems involving local charge ordering (beyond the Poisson–Boltzmann picture) in the present form. In principle, however, we can study such a problem by further extending our model to treat each ion as an individual fluid particle.

where e is the elementary charge. The electrostatic potential Ψ satisfies the Poisson equation,

$$\varepsilon\varepsilon_0\vec{\nabla}^2\Psi = -\rho_e, \quad (4)$$

where ε is the relative dielectric constant and ε_0 is the permittivity of space. The time evolution of the ion concentration field C_α is described by

$$\frac{DC_\alpha}{Dt} = \frac{\partial C_\alpha}{\partial t} + \vec{\nabla} \cdot (\vec{v}C_\alpha) = -\vec{\nabla} \cdot \vec{J}_\alpha, \quad (5)$$

where $\vec{J}_\alpha = -L_\alpha C_\alpha \vec{\nabla} \mu_\alpha$ is the flux of ion α induced by the gradient of the chemical potential μ_α . The mobility L_α of ion α is related to the diffusion constant D_α as $D_\alpha = k_B T L_\alpha$, where k_B is the Boltzmann constant and T is the temperature. The effective chemical potential μ_α is expressed as

$$\mu_\alpha = k_B T \ln C_\alpha + e Z_\alpha \Psi + k_B T \chi_\alpha \sum_i \phi_i. \quad (6)$$

Here the first term comes from the translational entropy of ions, the second one from the electrostatic contribution, and the third one from the penalty for the ions entering the inner region of the particles. χ_α is a kind of parameter describing the interaction between the ions and the particle, which is artificially introduced to prevent the ions from penetrating into the particles. The force field \vec{F} in equation (1) is expressed as

$$\vec{F} = \sum_i \frac{\vec{F}_i^{(0)} \phi_i}{\int d\vec{r} \phi_i} - \rho_e \vec{\nabla} \Psi. \quad (7)$$

Here the first term stems from the direct body force $\vec{F}_i^{(0)}$ acting on the particles as described before, while the second one stems from the electrostatic interaction. Note that $\vec{F}_i^{(0)}$ should not contain the Coulomb interaction since that is already included in the second term. For simplicity, we assume that the only non-electrostatic body force acting on particle i is the following steric repulsion from the other particles:

$$\vec{F}_i^{(0)} = \sum_{i \neq j} \vec{f}(\vec{r}_i - \vec{r}_j). \quad (8)$$

Here $\vec{f}(\vec{r})$ is the repulsive part of the Lennard-Jones interaction force, $\vec{f}(\vec{r}) = -(\partial/\partial\vec{r})V_0[(\sigma/|\vec{r}|)^{12} - (\sigma/|\vec{r}|)^6]$ with $|\vec{r}| < 2^{-1/6}\sigma$, where V_0 is the strength of the potential and σ is the range of interaction. We note that it is straightforward to include attractive interactions such as van der Waals interactions into $\vec{F}_i^{(0)}$, if necessary. Equations (1)–(8) together with the incompressibility condition $\vec{\nabla} \cdot \vec{v} = 0$ compose a set of electrohydrodynamic equations of charged colloidal suspensions. They are essentially the same as those found in the standard textbook [1, 2], except that the motion of the fluid particles and the resulting hydrodynamic flow are included.

To demonstrate the validity of our method, we apply it to a problem of electrophoretic deposition in charged colloidal suspensions. This problem is quite important both scientifically and technologically. Recently, the importance of the electrohydrodynamic interactions is suggested in conjunction with spontaneous cluster formation of particles upon their electrophoretic deposition onto an electrode [11–14]. The observed apparent long-range attraction between deposited particles having an equal charge is at variance with the intuition that equally charged particles should repel each other. The origin of such an attraction has been attributed as the electrohydrodynamic interaction. Anderson and co-workers analysed the electrohydrodynamic equations and calculated the flow profile about a single deposited

particle in a dc⁵ external electric field [15–17]. They showed that the resulting flow is directed toward a particle, so the flow can cause an attractive drag force on other particles.

Let us apply the above extended FPD model to the electrophoresis of charged colloids confined between two flat electrodes facing each other. We set the spatial axis z perpendicular to the electrodes, while the x and y axes are set parallel to them. For simplicity, we consider a two-dimensional (2D) problem. That is, we assume that the system is uniform along the y axis and thus the 2D circular particles that we deal with are cylinders that are forced to align along the y axis. The bottom electrode is set at $z = 0$ and the top one at $z = d$. Thus the gap between the two electrodes is d . We use the Dirichlet boundary condition for \vec{v} , Ψ , and \vec{J}_α at the electrodes: $\vec{v}(z = 0) = \vec{v}(z = d) = 0$, $\Psi(z = 0) = 0$, $\Psi(z = d) = V$, and $\vec{J}_\alpha(z = 0) = \vec{J}_\alpha(z = d) = 0$. For C_α , we use the Neumann boundary condition: $\partial C_\alpha / \partial z = 0$ at $z = 0$ and d . We also add the term $\sum_i \vec{f}_w(\vec{r}_i)$ to the rhs of the equation (8), where \vec{f}_w is the steric repulsion force acting on particle i from the two electrodes, whose functional form is set to be essentially the same as \vec{f} . We use the periodic boundary condition along the x direction as $g(x + L) = g(x)$, where g stands for all the field variables.

To solve equations (1)–(8) numerically, we discretize the space coordinate \vec{r} and the time variable t . In the calculation of the Navier–Stokes equation (see equation (1)), we set the lhs to be zero (Stokes approximation). This is justified since the Reynolds number $Re = \rho a v / \eta_s$ is quite small for aqueous suspensions of colloids of sub-micron size. For example, $Re \sim 10^{-4}$ for the particle of radius $a = 100$ nm with the electrophoretic mobility of $u = v/E \cong 1$ ($\mu\text{m s}^{-1}$) (V cm^{-1})⁻¹ under the electric field $E = 10^3$ V cm^{-1} . Thus the time integration should be carried out just for $\{\vec{r}_i\}$ and $\{C_\alpha\}$. We calculate their time evolution by using an explicit Euler integration for equations (2) and (5), respectively. In each time step, Ψ and \vec{v} are calculated using iteration methods. We calculate Ψ by solving equation (4) using a successive over-relaxation (SOR) scheme. For \vec{v} , on the other hand, we use a simple iteration procedure: $\vec{v} \rightarrow \vec{v} + \delta \times [\vec{F} - \vec{\nabla} p + \vec{\nabla} \cdot \eta \{ \vec{\nabla} \vec{v} + (\vec{\nabla} \vec{v})^T \}]$, where δ is a small positive constant. We repeat this iteration until the change in \vec{v} per iteration step becomes sufficiently small. In the calculation of $\vec{F} - \vec{\nabla} p + \vec{\nabla} \cdot \eta \{ \vec{\nabla} \vec{v} + (\vec{\nabla} \vec{v})^T \}$, we carry out an inverse Fourier transformation of $\vec{T}_q \cdot [\vec{F} + \vec{\nabla} \cdot \eta \{ \vec{\nabla} \vec{v} + (\vec{\nabla} \vec{v})^T \}]_q$ [10]. Here \vec{T}_q is the operator of the transverse projection in q space, which is specially modified such that \vec{v} satisfies the non-slip boundary condition at the walls.

In the present simulation, we fix the particle radius as $a = 20$ nm and the interfacial width as $\xi = 10$ nm. We assume that the particles are positively charged and the amount of charge of the particle cylinder is set to $20e$ per length of 10 nm. We employ 1:1 electrolyte as the bulk fluid and assume that the ions with a negative charge are identical to the counterions of the particles. We set $T = 300$ K. Although we can include the force noise term $\vec{\zeta}$ such that it satisfies the fluctuation-dissipation theorem, here we ignore it for simplicity⁶: thus, there are no random Brownian motions of particles in our simulations. The relative dielectric constant and the viscosity of the solvent are set to be $\varepsilon = 80$ and $\eta_s = 1$ cP, respectively. The viscosity of the fluid particles is set to be $\eta_c = 50\eta_s$, which is high enough for approximating the solid particles [10]. The diffusion constant D_α of the ions is set to be $D_\alpha = 10^{-5}$ $\text{cm}^2 \text{s}^{-1}$. We set the energetic penalty $k_B T \chi_\alpha$ for the ion penetrating inside the particle as $\chi_\alpha = 10$. The spatial coordinates are discretized by the regular mesh, whose size Δ is the same as ξ . The number of mesh points composing the system is $N_x \times N_z = 64 \times 32$; thus, the gap between the electrodes is $d = (N_z - 1)\Delta = 310$ nm and the repeating period in the x direction is $L = N_x \Delta = 640$ nm.

⁵ The detailed mechanism of the generation of the electrohydrodynamic flow is considered to differ between the dc electrical field case [15–17] and the ac one [18, 19].

⁶ Note that the drift motion of a particle ($\sim \text{mm s}^{-1}$) in our simulation is much faster than the diffusional motion.

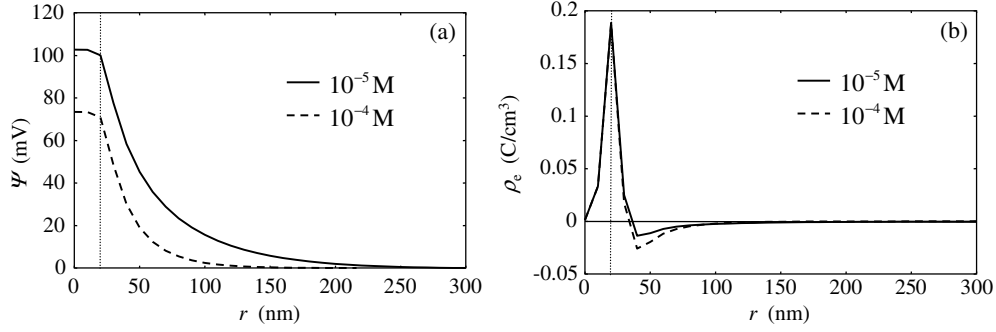


Figure 1. (a) The electrostatic potential profile and (b) the total charge density around the cylinder particle of radius $a = 20$ nm. The amount of charge on the cylinder is $20e$ per cylinder length of 10 nm. The relative dielectric constant is $\epsilon = 80$. The results for the two average concentrations of added 1:1 electrolyte, C , are shown: $C = 10^{-4}$ M (Debye length $\xi_D \approx 30$ nm) and $C = 10^{-5}$ M ($\xi_D \approx 100$ nm). The vertical dotted lines represent the position of the particle surface $r = a = 20$ nm. Other model parameters: $\chi_\alpha = 10$ and $\Delta = \xi = 10$ nm.

First we show the simulation results for the ion distribution about a charged particle in equilibrium. Figures 1(a) and (b) show the equilibrium electrostatic potential profile Ψ and the total charge density ρ_e , respectively. They are obtained for the steady state reached by the FPD simulation for a charged particle fixed in space. Although we use a quite large value for the interfacial width ($\xi = 10$ nm) as well as a rough discretization mesh ($\Delta = 10$ nm), the profiles of Ψ obtained are quite reasonable as long as the Debye length ξ_D is larger than $\xi = \Delta$. We also note that the artificial penalty term $k_B T \chi_\alpha \sum_i \phi_i$ in the ion chemical potential μ_α (see equation (6)) works well in preventing the ions from penetrating inside the particle; thus, a clear electric double layer is formed around the particle.

Next we consider the kinetic process of the electrophoresis of charged particles under the electric potential difference V between the electrodes. We initially equilibrate the ion distribution before applying the finite V . For the electrophoresis of a single particle, we have checked that the steady velocity v_∞ of the particle is proportional to the strength of the electric field $E = V/d$ for the range of E from 10^2 to 10^3 V cm $^{-1}$. The electrophoretic mobility $u = v_\infty/E$ estimated in these simulations is of the order of 1 ($\mu\text{m s}^{-1}$) (V cm $^{-1}$) $^{-1}$, which is consistent with the experimental values reported for charged colloids suspended in water.

Figure 2 depicts the kinetic process of the electrophoretic deposition of the two charged particles, which are initially put close to each other in the middle of the electrodes (i.e., at $z = d/2$). Let us index the left and the right particles as $i = 1$ and 2 , respectively. Figure 3 shows the temporal changes in the particle separation $x_2 - x_1$ and the vertical position $z = z_1 = z_2$ for the same simulation. During the electrophoretic migration toward the bottom electrode, the particles first repel each other due to the electrostatic repulsion between them (note that $\xi_D \approx 100$ nm for this case). However, just before the particles are deposited on the electrode, they begin to apparently attract each other. We can see in figure 2 that this counter-intuitive behaviour is induced by the upward flow through the Debye layer around the particles, which is driven by the electrical field. This flow causes the hydrodynamic drag force along the bottom electrode, which pulls a particle toward another.

Thus, the apparent attractive interaction is purely of kinetic origin. The particles approach each other when this electrically driven hydrodynamic drag force overwhelms the electrostatic repulsion. In the final stage (see figure 2(d)), we can note that the ion concentration between the particles becomes quite high due to the strong overlap of the Debye layers. The resulting repulsive interaction is balanced with the electrohydrodynamic drag force in the steady state.

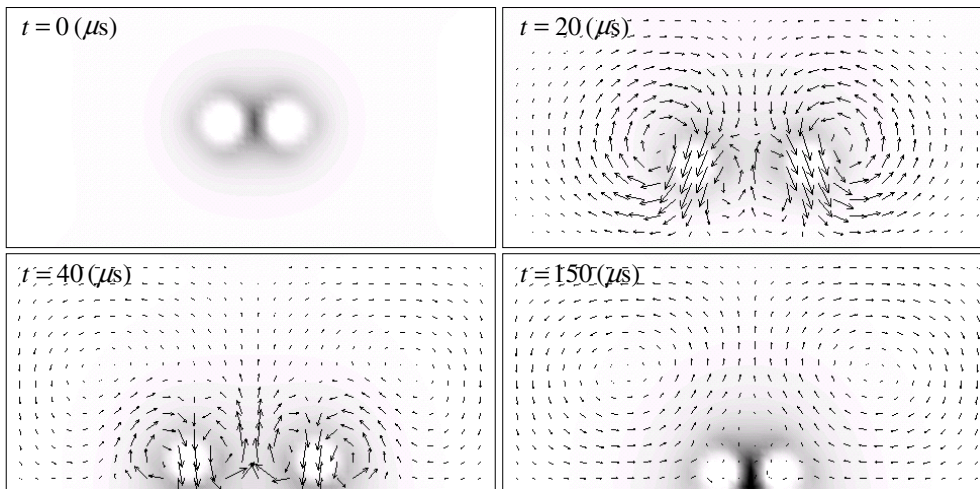


Figure 2. Snapshots of the process of the electrophoretic deposition of two charged particles placed between the electrodes. The density plot represents the counterion concentration. The arrows indicate the velocity field. The electrodes are separated by 310 nm ($d = 310$ nm). The applied voltage is $V = 100$ mV. The average concentration of the added salt is 10^{-5} M.

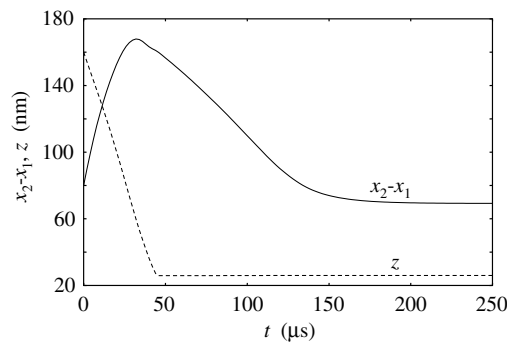


Figure 3. The separation between the particles ($x_2 - x_1$) and their vertical position ($z = z_1 = z_2$) as a function of time t in the same calculation as shown in figure 2.

We have also investigated how two deposited particles with an initial separation of 200 nm move along the electrode to approach each other, focusing on the dependences on the salt concentration C and the applied voltage V . The results are shown in figure 4. The stronger the electric field applied, the faster the approach speed becomes. We can also note that the greater the amount of salt added or the stronger the electric field applied, the shorter the interparticle distance in the final stationary state becomes.

Let us consider what controls this approach kinetics and the final stationary state. In this process, the electrostatic repulsion and the hydrodynamic force generated by electroosmotic flow are competing. The former is not effective when the interparticle separation is larger than the Debye length ξ_D , since it is screened by the diffuse electric double layer formed by the counterions. The latter is, on the other hand, caused by the convective flow induced by the electrically driven ions, whose flow field is approximately dipolar. When the interparticle separation $r (=x_2 - x_1)$ is longer than ξ_D , thus, the particle velocity, which should

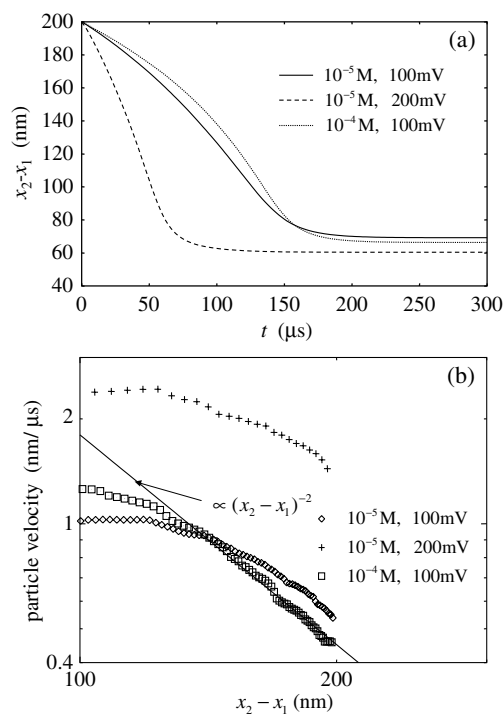


Figure 4. (a) Separation distance $x_2 - x_1$ between a pair of particles on the electrode as a function of time t for different applied voltages and salt concentrations. Initially, the separation between the two particles is set to be 200 nm. (b) A double-logarithmic plot of the particle velocity against $x_2 - x_1$. The solid line has a slope of -2 .

be proportional to the velocity of the lateral flow, should decay as r^{-3} for a 3D system [13]. For a 2D system, we expect it to decay as r^{-2} . We do indeed confirm this power law decay for $C = 10^{-4}\text{ M}$ and $V = 100\text{ mV}$, as shown in figure 4(b). For the case of $C = 10^{-5}\text{ M}$, such a distinct power law behaviour cannot be observed except for a narrow region where $x_2 - x_1 \gg \xi_D$ (see figure 4(b)) because the Debye length ($\xi_D \approx 100\text{ nm}$) is comparable to half of the surface separation between the particles that we examined; for this case we have to take the effect of the electrostatic repulsion into account and the above simple scaling argument no longer holds. Because of the dipolar nature, the flow near the wall has a lateral component, which produces the drag force from a particle toward another one. The strength of this flow should increase with increasing ion flux J and Debye length ξ_D . The increase in the electric field E leads to the increase in J , which should result in a faster approach speed. This is consistent with what is shown in figure 4(a). On the other hand, the effect of the salt concentration C is subtle since it increases J but decreases ξ_D . Next we consider the final steady state, which is a result of the competition between the electro-osmotic force and the Coulomb repulsion. The above arguments concerning the roles of E and C in the electrohydrodynamic force should also apply to the interparticle separation in the stationary state. In addition, we also have to consider the fact that the increase in C weakens the electrostatic repulsion, which results in a decrease in the final separation. Thus, we expect the interparticle separation to decrease with increasing E and/or C , consistently with what is shown in figure 4(a). In previous studies [16, 17], the effects of the thermal Brownian motion of particles on the approach process were discussed while neglecting the electrostatic interaction, which we take into account here. More detailed

studies on the dependences on C and E under the influence of thermal force noises will be shown elsewhere.

In summary, we have developed a new simulation method to deal with the dynamics of charged colloidal suspensions while including full hydrodynamic and electrostatic interactions among charged colloidal particles, ion clouds, and liquid. The validity of this method has been demonstrated for the problem of electrophoretic deposition kinetics. The electrostatic and the hydrodynamic interactions as well as the electro-osmotic effect are naturally introduced in the simulation. Although we have shown a two-particle simulation of a small system size in two dimensions, it is quite straightforward for our method to treat a many-particle system and/or a three-dimensional system. We hope that our new method will contribute to a deeper understanding of kinetic aspects of complex many-body problems in charged colloidal suspensions.

The authors (HK and HT) acknowledge the support from the Ministry of Education, Science and Culture, Japan (Grant-in-Aid for Scientific Research Nos 13554001 and 14204038), respectively. We also acknowledge the OCTA2002 (<http://octa.jp>), whose class files are used for solving the Poisson equation (4).

References

- [1] Hunter R 1986 *Foundation of Colloid Science* (Oxford: Clarendon)
- [2] Russel W B, Saville D A and Schowalter W R 1989 *Colloidal Dispersions* (Cambridge: Cambridge University Press)
- [3] Lowen H, Allahyarov E, Likos C N, Blaak R, Dzubiella J, Jusufi A, Hoffmann N and Harreis H M 2003 *J. Phys. A: Math. Gen.* **36** 5827
- [4] Tanaka M and Grosberg A Y 2002 *Eur. Phys. J.* **7** 371
- [5] Brady J F, Phyllips R J, Lester J C and Bossis G 1988 *J. Fluid. Mech.* **195** 257
- [6] Foss D R and Brady J F 2000 *J. Fluid. Mech.* **407** 167
- [7] Lowen H 1992 *J. Phys.: Condens. Matter* **4** 10105
- [8] Allahyarov E, Löwen H and Trigger S 1998 *Phys. Rev. E* **57** 5818
- [9] Ohshima H 1997 *J. Colloid Interface Sci.* **188** 481
- [10] Horbach J and Frenkel D 2001 *Phys. Rev. E* **64** 061507
- [11] Tanaka H and Araki T 2000 *Phys. Rev. Lett.* **85** 1338
- [12] Bohmer H 1996 *Langmuir* **12** 5747
- [13] Trau M, Saville D A and Aksay I A 1996 *Science* **272** 706
- [14] Yeh S-R, Seul M and Shraiman B I 1997 *Nature* **386** 57
- [15] Trau M, Saville D A and Aksay I A 1997 *Langmuir* **13** 6375
- [16] Solomentsev Y, Bohmer M and Anderson J L 1997 *Langmuir* **13** 6058
- [17] Guelcher S A, Solomentsev Y and Anderson J L 2000 *Powder Technol.* **110** 90
- [18] Solomentsev Y, Guelcher S A, Bevan M and Anderson J L 2000 *Langmuir* **16** 9208
- [19] Sides P 2001 *Langmuir* **17** 5791
- [20] Nadal F, Argoul F, Hanusse P, Pouligny B and Ajdari A 2002 *Phys. Rev. E* **65** 061409